Front. Phys., 2014, 9(1): 82–89
DOI 10.1007/s11467-013-0395-8

RESEARCH ARTICLE

Experimental observations of ferroelectricity in double pyrochlore $Dy_2Ru_2O_7$

Zai-Chun Xu, Mei-Feng Liu, Lin Lin, Huimei Liu, Zhi-Bo Yan, Jun-Ming Liu†

Laboratory of Solid State Microstructures, Nanjing University, Nanjing 210093, China

Corresponding author. E-mail: †*liujm@nju.edu.cn*

Received August 20, 2013; accepted September 25, 2013

Double pyrochlore $Dy_2Ru_2O_7$ is synthesized and its magnetism and ferroelectricity below the Ru^{4+} spin ordering temperature (∼100 K) are investigated. The ferroelectric transition appears at ∼18 K, much higher than the Dy^{3+} spin ordering point at ∼1.8 K and lower than the Ru^{4+} spin ordering point at ∼100 K. The measured electric polarization at ∼2 K is as big as 145 μC/m^2 in the polycrystalline samples. It is argued that the ferroelectricity is possibly ascribed to the electric dipole ordering arising from the collective monopole excitations in the Dy^{3+} tetrahedrons in prior to the Dy^{3+} spin ordering into spin-ice like state below ∼1.8 K.

Keywords pyrochlore oxides, multiferroics, magnetically induced ferroelectricity

PACS numbers 75.85.+t, 77.80.-e, 75.50.Ee, 14.80.Hv

1 Introduction

The $A_2B_2O_7$ pyrochlore oxides, where A is a trivalent rare-earth ion and B is a tetravalent transition metal ion, have been receiving continuous attentions recent years due to the fascinating magnetic structures and frustrated interactions, as identified in many such oxides [1–4]. This allows these oxides to be the central objects for understanding the physics of spin frustration and fluctuations in condensed matters. In particular, the spin-ice/spin-liquid behaviors and magnetic monopole scenario as attractive issues have been intensively investigated [3, 4]. It is generally believed that these magnetic properties have the common structure origins. The lattice consists of two independent networks of corner-sharing tetrahedra with A ions and B ions occupying the tetrahedron corner sites respectively, as shown in Fig. 1(a) for $Dy_2Ru_2O_7$ as an example which will be addressed in this work [5]. Usually, the crystal field arising from, e.g. the B sublattice originated molecular field and the oxygen ions close to the A site imposes strong control of the orientation of the A site rare-earth 4*f* spins, aligning them along the local ⟨111⟩ directions like Ising spins [6]. Upon either magnetic A or B ion, the lattice is spin-frustrated and the magnetic structure can be highly degenerate even only the nearest- and next-nearest neighboring interactions are considered [7, 8]. In fact, the long-range dipole–dipole interaction, the strong crystal field effect, and the spin–orbit coupling (SOC), are found to play non-negligible roles [3, 4]. For example, when B species is a Ti or Sn ion, $Ho_2Ti_2O_7/Dy_2Ti_2O_7$ are spin ices while $Gd_2Ti_2O_7/Gd_2Sn_2O_7$ can be considered as nearly isotropic Heisenberg antiferromagnets [3, 4, 9–11]. In some other cases, the spin liquid behaviors are observed. If both A ion and B ion are magnetic, the magnetic frustration can be even more complicated because the A–B interactions are probably important. The representative materials are those $A_2B_2O_7$ pyrochlore oxides with 4*d* transition metal ion such as Ru^{4+} and Mo^{4+} at B sites and magnetic rare-earth at A sites [12–15], while the 4*d* transition metal ions usually have strong SOC effect. They are often referred as the double pyrochlore oxides.

One of the attractive and emergent phenomena in these $A_2B_2O_7$ pyrochlore compounds is ferroelectricity. For the cases where magnetic rare-earth ions at A sites are involved, these compounds may exhibit multiferroicity which accommodates the ferroelectric and magnetic orders simultaneously and the coupling between them [16–19], if the ferroelectricity is available. Nevertheless, so far synthesized compounds in this category have high lattice symmetry with space group $Fd\text{-}3m$ over the whole temperature (T) range, and no lattice symmetry breaking is generally believed, although the complicated interactions do allow a spatial symmetry breaking in these compounds [20]. Consequently, no possibility for conventional displacive-type ferroelectricity in these oxides would be expected. However, recent years, tremendous

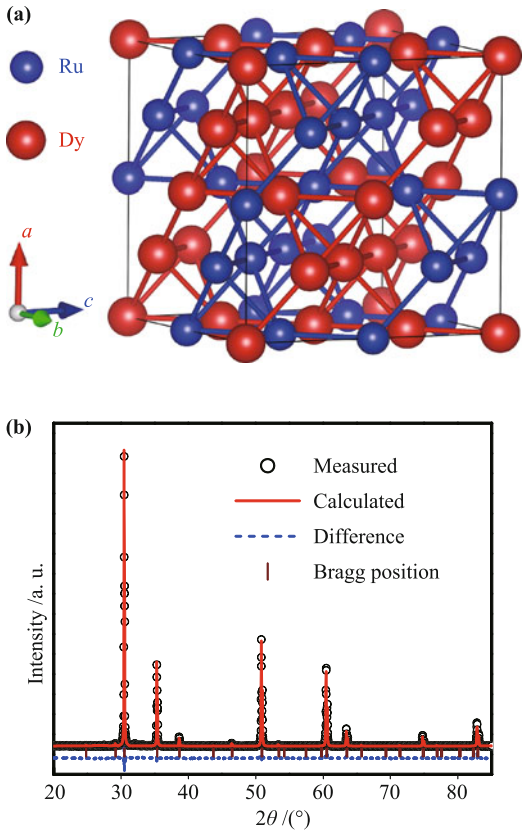

Fig. 1 **(a)** Schematic of lattice structure of DRO where the small blue solid spheres refer to Ru ions and the large red solid spheres to Dy ions. For clarity, the oxygen ions are omitted. **(b)** Measured θ–2θ XRD spectrum of a polycrystalline DRO sample where the Rietveld refined XRD data (Calculated) together with the labeled Bragg positions are inserted.

progresses in discovering a number of multiferroics have been made [16–19]. For these multiferroics, the ferroelectricity is associated with some specific spin orders and induced by specific magnetic interactions [21]. The electric polarization can have both electronic and ionic contributions, and the proposed microscopic mechanisms include the asymmetric exchange striction associated with the SOC via the Dzyaloshinskii–Moriya (DM) interaction and symmetric exchange striction associated with the spin–lattice coupling [16–19].

It should be pointed out that for the two types of microscopic mechanisms, the spatial symmetry breaking does occur but the coherent ionic displacements over the whole lattice as identified in normal ferroelectrics seem to be beyond the resolution of conventional structural characterization techniques. This is the reason for small electric polarization and low ferroelectric Curie temperature. Even so, these progresses enlighten substantial and continuous efforts in searching for ferroelectricity from those magnetic insulators with specific spin structures.

In fact, experimental observations of ferroelectricity in $A_2B_2O_7$ pyrochlore compounds such as $Ho_2Ti_2O_7$ and then $Gd_2Ti_2O_7$ have been reported recently [22–24]. Regarding the microscopic mechanism responsible for polarization generation in these compounds, Khomskii recently proposed an alternative scenario in which the magnetic monopoles as a result of the spin excitation at finite T simultaneously carry magnetic charges and electric dipoles [25]. A single spin tetrahedron allows the 3-in/1-out or 3-out/1-in spin configuration which can produce an electric dipole along the local $\langle 111 \rangle$ direction. These electric dipoles may align in a well ordered manner upon the energy partition, and thus a macroscopic polarization becomes possible.

It is understood that in the Khomskii model, the monopole excitation is the core ingredient of physics for this magnetically driven ferroelectricity. The magnitude of the as-carried electric dipoles depends on the SOC and the on-site Coulomb interaction U [25]. A strong SOC benefits to the magnitude enhancement, while the consequence of varying U seems unclear. This physics stimulates us to explore more ferroelectric candidates in $A_2B_2O_7$ pyrochlore oxides, in particular those pyrochlore oxides with $4d$ transition metal ion such as Ru^{4+} and Mo^{4+} etc. at B site, while the $4d$ B ion usually offers a SOC much stronger and weaker U than the $3d$ ions. In fact, quite a number of works addressing the magnetic ordering in double pyrochlore oxides (A=Gd, Tb, Dy, Ho etc., B=Ru) have been reported and particulars were identified in addition to some common characteristics [12–15, 26–28]. It is our priority to explore these materials for ferroelectricity, noting that so far no report on the ferroelectricity in such double pyrochlore oxides has been available.

In this work, we choose $Dy_2Ru_2O_7$ (DRO) for our investigation, noting that the magnetic properties and relevant phase transitions in DRO, $Ho_2Ru_2O_7$, $Yb_2Ru_2O_7$, and $Tb_2Ru_2O_7$ etc., were once investigated extensively [14, 15, 26–28]. Our experiment will demonstrate the ferroelectricity of DRO, whose microscopic origin is believed to be relevant with the Dy^{3+} spin ordering coupled with the Ru^{4+} sublattice.

2 Experimental details

The polycrystalline DRO samples were prepared by conventional solid-state sintering method. The stoichiometric amount of high-purity Dy_2O_3 and RuO_2 oxides was mixed and thoroughly ground for 48 hrs, and sintered in air at 1250°C–1400°C for 16 hrs each, with several intermittent heating- and grinding-steps. This sintering procedure has to be optimized, due to the preferential

evaporation of Ru during the sintering, so that the as-sintered samples are stoichiometric and the volume density is higher than 0.95 of the theoretical value.

The crystallinity of the as-prepared samples was checked using X-ray diffraction (XRD) (Bruker Corporation) equipped with Cu K_α radiation at room temperature, assisted by careful lattice structure characterization using the Rietveld refining method. In addition, we performed X-ray photoelectron spectroscopy (XPS) measurements on the chemical composition and species valences of the samples and only those stoichiometric samples were chosen for subsequent characterizations. The *dc* magnetic susceptibility under zero-field cooled (ZFC) and field-cooling (FC) conditions with a measuring/cooling field of 1000 Oe, as well as specific heat, were probed respectively using the Quantum Design Superconducting Quantum Interference Device (SQUID) and Physical Properties Measurement System (PPMS) in the standard procedures down to $T = 2$ K.

For the dielectric and polarization measurements, the samples were cut into standard pellets of 10 mm in diameter and 0.2 mm in thickness and then sputtered on the two surfaces with Au electrodes. The dielectric susceptibility was measured using the HP 4294A impedance analyzer and the polarization was evaluated by measuring the pyroelectric current upon the warming process. Both measurements were performed in measuring system connected with the PPMS apparatus. For this pyroelectric current probing, the samples were cooled down to $T = 2$ K from 60 K under a poling field of $E = 10$ kV/cm and then short-circuited at $T = 2$ K for 30 min. Then the samples under no electric bias were warmed up at a rate of 2 K/min during which the current released from the sample was collected. This current was also measured under warming rates of 4 K/min and 6 K/min, and the three sets of data were compared to insure no contribution from sources other than the pyroelectric current. The same procedure was repeated at $E = -10$ kV/cm for checking the polarization reversal, and at $E = 10$ kV/cm under various magnetic field H for checking the response of polarization against H, i.e., the magnetoelectric coupling effect.

3 Results and discussion

3.1 Magnetic behaviors and specific heat

The measured XRD θ–2θ pattern is shown in Fig. 1(b), referring to the lattice structure given in Fig. 1(a). Meanwhile, the Rietveld refined XRD data using the GSAS program are inserted for comparison (Calculated). Very small difference between the measured and calculated data is shown. The reliability of the Rietveld refinement is demonstrated by the high-quality refinement parameters $R_p = 2.83\%$ and $R_{wp} = 3.90\%$. The lattice parameters at room temperature as obtained by the refinement are $a = b = c = 1.015$ nm, consistent quite well with earlier reports [12–15].

The measured *dc* magnetic susceptibility χ as a function of T under the ZFC and FC conditions is shown in Fig. 2(a), where the dependence of χ^{-1} against T is plotted. The measured C_P as a function of T is presented in Fig. 2(b). A fit of the data in the high T range ($T > 120$ K) using the Curie–Weiss law: $\chi^{-1}(T) \sim (T - \Theta_{\rm CW})$, yields an antiferromagnetic (AFM) Curie–Weiss temperature $\Theta_{\rm CW} = -10 \pm 2$ K and a paramagnetic moment of $\sim 10.2\mu_{\rm B}$. This moment is comparable roughly with the free ion value appropriate for the $^6{\rm H}_{15/2}$ Dy^{3+} ion plus the Ru^{4+} ion with a spin moment of only $\sim 1.0\mu_{\rm B}$, indicating that the paramagnetic state dominates above $T = 120$ K, consistent with earlier reports [28], while this estimation may not be of quantitative sense. It is seen that a weak separation between the ZFC and FC χ^{-1}–T curves appears at $T = T_{\rm Ru} \sim 100$ K, as shown in the inset of Fig. 2(a), indicating a magnetic transition at this temperature. Correspondingly, a clear λ-type anomaly in the C_P–T curve at $T_{\rm Ru}$ is seen, indicating that this magnetic transition is of second-order.

The physical origin for this magnetic transition is not yet well understood. Obviously, this transition is relevant with the long-range Ru^{4+} spin ordering due to the very strong Ru–Ru interaction, as well documented in literature for $Y_2Ru_2O_7$ and $Lu_2Ru_2O_7$ in which Ru^{4+} is the only magnetic species [14, 15]. In fact, for most cases, the temperature for spin ordering of magnetic rare-earth ions in transition metal oxides cannot be as high as 100 K and most likely it is below 10 K, although there is indeed exceptional case. This behavior also indicates that the long-range spin correlation builds up at $T_{\rm Ru}$. This Ru^{4+} spin ordered state is characterized by a noncollinear spin structure and each spin is roughly perpendicular to the local [111] direction of the tetrahedron unit [26]. Subsequently, the difference between the χ^{-1}–T curves for the ZFC and FC cases becomes gradually disappeared with decreasing T down to 2 K, the lowest temperature in the present experiment, and no additional spin ordering occurs at $T > 2$ K.

However, it is noted that the measured C_P which falls down gradually with decreasing T begins to turn back at $T = T_{\rm c} \sim 16$ K where the C_P reaches the minimum. For reference, we insert in Fig. 2(b) the C_P–T data down to $T = 0.4$ K taken from Ref. [28]. One sees that our data

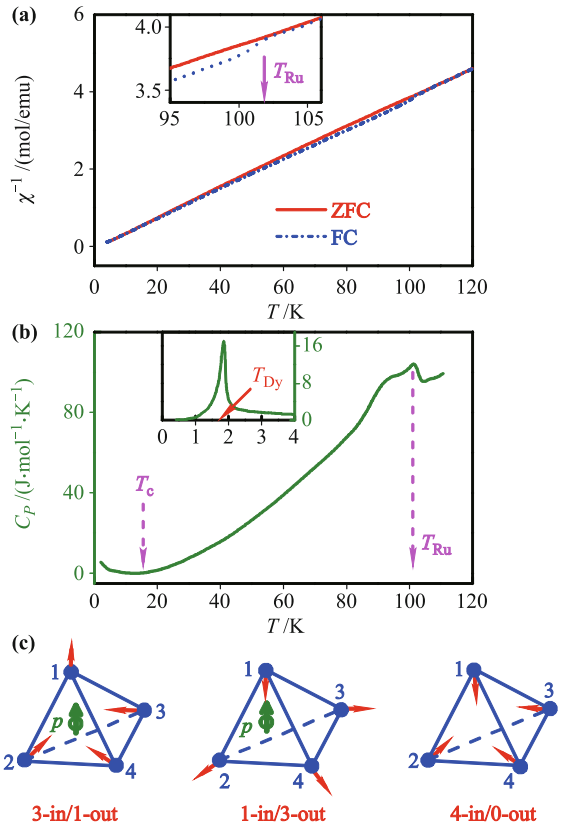

Fig. 2 **(a)** Measured inverse magnetic susceptibility χ^{-1} under the ZFC and FC conditions and **(b)** specific heat C_P as a function of T respectively. The insert specific heat data are taken from Ref. [28]. **(c)** Three of the possible excitation modes of the spin ice structure in one tetrahedron unit: 3-in/1-out, 1-in/3-out, and 4-in/0-out.

at the low-T end coincide with the data from literature. It was reported that the sharp peak at $T = T_{Dy} \sim 1.8$ K is a symbol of the second-order phase transition, characterizing the Dy^{3+} spin ordering although the details of the spin structure below T_{Dy} is still under debate. The estimated entropy change from the C_P-peak is much bigger than that for a typical spin ice transition [28], but other researches indicated the Dy^{3+} spins favor the spin ice like state [14, 15].

To this stage, the puzzling issue is the spin relaxation in $T_{Dy} < T < T_c \sim 16$ K, as reflected by the up-turn of C_P with decreasing T. This relaxation should be related to the pre-ordering of the Dy^{3+} spins coupled with the high-T Ru^{4+} spin order [28]. Above T_c, the long-range Dy^{3+} spin order is not yet well developed. At such low T-range, all the ions in the lattice, in particular the two oxygen ions very close to Dy^{3+} ion in each tetrahedron unit (somehow similar to the H_2O tetrahedron unit) imposes sufficiently strong crystal field effect on the Dy^{3+} spins, enforcing them to align along the local [111] direction like Ising spins. This effect becomes more pronounced at lower T, and thus it is believed that the Dy^{3+} spin relaxation right above T_{Dy} is dominant with the local "2-in/2-out", "3-in/1-out", "3-out/1-in" configurations, plus minor "4-in" and "4-out" ones, in terms of the single spin tetrahedron unit. The "3-in/1-out" and "3-out/1-in" configurations can be seen as the excitation modes of the spin ice structure, with magnetic monopole-antimonopole pair connected by a Dirac string. An electric dipole together with a magnetic charge is associated with each of the monopoles and antimonopoles, as schematically shown in Fig. 2(c) for three of these modes. A sufficiently high density of such electric dipoles allows efficient interaction between them, probably resulting in macroscopically measureable electric polarization.

3.2 Electric polarization

Given the above discussion on the magnetic structure and the possibility for electric dipole generation, one has reason to expect the non-zero electric polarization in DRO.

The measured dielectric susceptibility ε at 10 kHz and pyroelectric current I_P as a function of T respectively are shown in Figs. 3(a) and (b). As usual, the measured $\varepsilon(T)$ below $T = 30$ K decreases continuously with decreasing T, but a weak broad peak appearing at $T = T_\varepsilon \sim 18$ K is observed. This peak roughly coincides with the up-turn point $T_c \sim 16$ K in the $C_P(T)$ curve [Fig. 2(a)] and we treat them as T_c hereafter, suggesting a possible ferroelectric phase transition at T_c. Besides this broad peak, the measured dielectric dispersion on frequency is relatively weak and the data at low frequency show big fluctuations.

The electric polarization as evaluated from the pyroelectric current method is often questioned since the collected current signals may include contributions from sources other than the polarization current. For checking this matter, we measure the current signals at three different warming rates (2, 4, 6 K/min) and the data are shown in Fig. 3(b). It is seen that the three curves peak exactly at $T \sim 12$ K with no shifting towards the high-T side for higher warming rate. In fact, the three sets of data, times respectively by the warming rate, almost overlap with each other. No shifting of the peak upon different warming rates implies that the current does come from the pyroelectric effect [$I_P(T)$] associated with the ferroelectric phase transitions, and otherwise thermally activated signals from defects-trapped charges on the interfaces or inside the sample would exhibit a shift of the peak. No electric bias on the sample is noted. This methodology has been well recognized and it is especially useful for low-T cases [29–31]. In addition, it is noted that for an insulating oxides under zero electric

bias, a thermally stimulated current of 10 pA for a capacitor of 10 mm^2 in electrode area at $T \sim 10$ K may be too big to be possible.

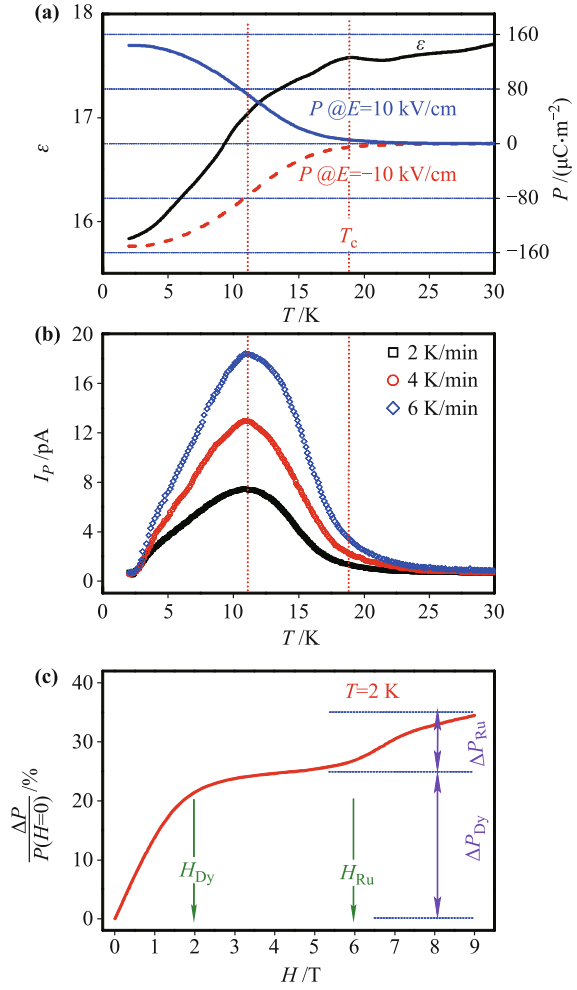

Fig. 3 **(a)** Measured dielectric constant ε at frequency of 10 kHz and evaluated electric polarizations P under $E = \pm 10$ kV/cm as a function of T respectively. **(b)** Measured pyroelectric currents I_P at three different warming rates (2, 4, and 6 K/min) as a function of T. **(c)** Evaluated polarization variation $\Delta P/P(H = 0)$ at $T = 2$ K as a function of T.

From the $I_P(T)$ data, the evaluated polarization $P(T)$ is plotted in Fig. 3(a), indicating the transitions occurring around T_c. The saturated polarization at $T < 5$ K reaches up to 145 μC/m^2 and much larger polarization is expected for single crystal sample. Even so, this value of polarization is much smaller than that for normal ferroelectrics. In addition, our measurement confirms that this polarization is reversible, with the measured $P(T)$ under negative poling field $E = -10$ kV/cm plotted in Fig. 3(a) for comparison. Our pyroelectric current data evidence the ferroelectricity in DRO, which has never been reported earlier. And more, the electric polarization is comparatively large with respect to those typical type-II multiferroics [16–19], implying that DRO is a promising multiferroic material.

Additional evidence is given by the measured $P(T)$ data under varying magnetic field H. It is seen that magnetic field H gradually suppresses the polarization over the whole T-range, indicating the remarkable response of P against H. Interestingly, evaluating the $P(H)$ data gives more features, as shown in Fig. 3(c) where $\Delta P/P(0) = 1 - P(H)/P(0)$ is plotted against H. In the low-H field, $\Delta P/P(0)$ shows a rapid growth and then reaches a plateau at $H \sim H_{Dy} = 2$ T until $H \sim H_{Ru} = 6$ T. At $H > H_{Ru}$, a second growth of $\Delta P/P(0)$ is identified. Unfortunately, data at even higher H are unavailable to us due to the apparatus limit. This two-stage feature of $P(H)$ response probably reflects two components for the electric polarization, which are respectively responsible for ΔP_{Dy} and ΔP_{Ru} as defined in Fig. 3(c), to be discussed below.

With respect to the ferrielectric evidences given above, two issues regarding the ferroelectric transitions should be addressed here. First, the dielectric anomaly at T_c is far from significant as that for normal ferroelectrics. For typical multiferroics, the electric polarization is small and has electronic contribution and ionic contribution. The ionic polarization arises from a typical displacive transition usually featured with a sharp dielectric anomaly, but it is not the case for the electronic polarization. In most cases, the single crystal samples show a typical 0.05%–10% change in dielectric constant at the transition point, while this value is several or tens times smaller in polycrystalline samples.

Second, no anomaly in the $C_P(T)$ spectrum for this ferroelectric transition is observed. It is well known that for magnetic oxides, the main contribution to the specific heat at low temperature range can be magnetic, i.e., the spin fluctuations and ordering dominate the specific heat signals. This is the reason why the specific heat anomalies at the Ru spin ordering and Dy spin ordering can be clearly observed, as shown in our results. So far all specific heat data on $R_2Ru_2O_7$ and $R_2Ti_2O_7$ (R is rare-earth) have been explained from the spin fluctuations and ordering. This indicates that the lattice contribution is weak with respect to the magnetic contributions. In fact, for DRO, the measured electric polarization is so small that the lattice fluctuations arising from the ferroelectric transition is too weak to be observable.

3.3 Magnetic monopole excitations for ferroelectricity

We start from the magnetic phase transitions to discuss the microscopic mechanisms for the polarization generation in DRO. It is revealed that the Ru^{4+} spins order at

$T_{Ru} \sim 100$ K. In this spin ordered state, it seems that no polarization is generated although the Ru^{4+} spins align in slightly non-collinear pattern. As discussed in Section 3.1, below T_{Ru}, no clear magnetic transition until $T_{Dy} = 1.8$ K at which the Dy^{3+} spins order into the spin ice like state occurs. Nevertheless, the ordering sequence of Dy^{3+} and Ru^{4+} spins is not so simple, and in fact the Dy^{3+} spins may have the pre-transitions into the spin ice like state at $T_c \sim 18$ K, as inferred from the published data [28, 32]. Due to the strong crystal field effect of the lattice ions on the Dy^{3+} spins, one may be allowed to argue that the Dy^{3+} spins tend to align along their local [111]-axes like the Ising spins and develop the spin ice like ordered domains between T_{Dy} and T_c, although relevant evidence is somehow required. This alignment may be realized by the slow (single) Ising-like spin relaxations [32], so that eventually an ordered domain is developed. In this T-range, the spin monopole excitation from these domains contributes to electric dipole following the mechanism proposed by Khomskii [25]. These electric dipoles interact with each other, resulting in the ferroelectric transitions at T_c, responsible for the observed polarization in DRO. This scenario is schematically illustrated in Fig. 4, where the $C_P(T)$ curve is re-plotted in Fig. 4(a) and the proposed Ru^{4+} and Dy^{3+} spin sub-lattices at three different T-ranges, I, II, and III, are shown in Figs. 4(b) and (c), respectively. In the three ranges, the Ru^{4+} and Dy^{3+} spin states are labeled as inserts in Fig. 4(a) respectively.

The above scenario seems to indicate that the Dy^{3+} spin ordering is the unique origin for the ferroelectricity. Nevertheless, it is understood that the Ru^{4+}–Dy^{3+} interaction may take effect below T_c with respect to thermal fluctuations, as reflected by the spin relaxation process between T_{Dy} and T_c. In this case, any change of the Ru^{4+} spin configuration is believed to modulate the Dy^{3+} spin state too. This Ru^{4+}–Dy^{3+} interaction is one of the key ingredients for the $P(H)$ response. Given the fact that the rare-earth $4f$ spin interaction is weak and a magnetic field of several Tesla is usually sufficient to break the $4f$ spin order, one understands that the rapid growth of $\Delta P/P(0)$ in the low-H regime below $H_{Dy} \sim 2.0$ T, as shown in Fig. 3(c), arises from the H-induced suppression of the pre-transitions of the Dy^{3+} spins below T_c and the spin ice like state below T_{Dy}. A field of $H = H_{Dy} \sim 2.0$ T is believed to reverse partially the Dy^{3+} spins from the alignment along the local [111] directions to other [111] directions with which the lattice has lower magnetic static energy. This corresponds to the first growth stage of $\Delta P/P(0)$ shown in Fig. 3(c). The measured M–H loop at low T such as 5 K, plotted in Fig. 5, confirms this argument and the magnetization

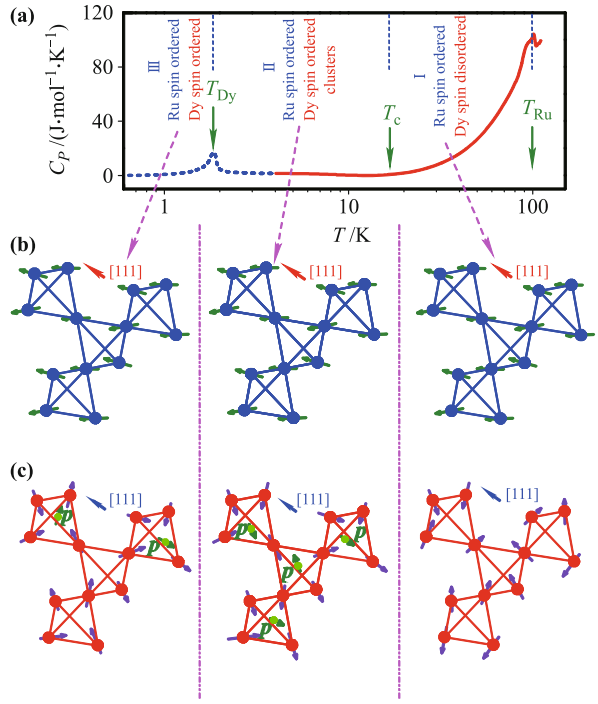

Fig. 4 **(a)** Measured specific heat $C_P(T)$ where the dash line is taken from Ref. [28], and the suggested three T-ranges in which different Dy^{3+} and Ru^{4+} spin configurations are labeled. The proposed Ru^{4+} spin configurations **(b)** and Dy^{3+} spin configurations **(c)** corresponding to the three T-ranges are plotted, where the electric dipole p associated with each Dy^{3+} spin tetrahedron unit is shown.

is already saturated at $H > 2.0$ T, noting that the M is mainly contributed from the Dy^{3+} spins. Possibly, a much higher magnetic field is needed to align all these spins to be along the magnetic field.

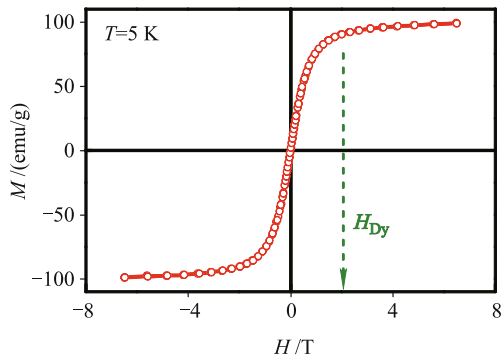

Fig. 5 Measured M–H hysteresis at $T = 5$ K. The magnetization M becomes saturated at $H = H_{Dy} \sim 2$ T.

However, as mentioned earlier, the Ru^{4+}–Ru^{4+} interaction is very strong and it also contributes to the strong crystal field effect on the Dy^{3+} spins. A field H as low as 2.0 T is far from sufficient to break the non-collinear AFM Ru^{4+} order, and thus a complete ferromagnetic alignment of all the Dy^{3+} spins would be impossible un-

less the Ru^{4+} spins are enforced to the parallel alignment under sufficiently high magnetic field. This field seems to be larger than $H_{Ru} = 6.0$ T, and thus the Ru^{4+} spins begin to reverse, leading to associated reverse of the Dy^{3+} spins. This corresponds to the second growth stage of $\Delta P/P(0)$ that begins at $H > H_{Ru} \sim 6.0$ T, as shown in Fig. 3(c).

3.4 Discussion

The above model seems to reasonably explain the observed magnetically induced ferroelectricity in DRO. However, a thorough understanding of the underlying mechanism requires additional investigations. First, the spin ice like order of the Dy^{3+} spins below T_{Dy} is believed, but no sufficient evidence has been available, and neutron scattering experiment becomes challenging due to the strong absorption of neutrons by Dy ions.

Second, our ferroelectric measurement has not yet reached down to even lower value than T_{Dy}. If the Dy^{3+} spins follow strictly the "2-in/2-out" order, no electric dipole is possible for the spin ice tetrahedron and thus no ferroelectricity below T_{Dy} is expected. Surely, the spin ice state also accommodates large configuration entropy and such a strict "2-in/2-out" order over the whole lattice may not be possible even at the lowest temperature. It is also implied that the transitions between the "2-in/2-out" configuration and the "3-in/1-out"/"1-in/3-out" configurations are easy. In this case, non-zero polarization in range III would be observable. Furthermore, for the electric polarization measurement, the sample is under an electric poling (E) during the cooling sequence. The electro-static energy ($-P \cdot E$) favor the "3-in/1-out"/"1-in/3-out" configurations because they carry magnetic monopoles and electric dipoles. Therefore, such a poling favors a high-density of magnetic monopoles.

Third, the relaxation behavior of Dy^{3+} spins in between T_{Dy} and T_c remains to be an issue, although the present experiment correlates it with the pre-transitions from the paramagnetic state to a quasi spin-ice state with high density of magnetic monopoles. Finally, the Ru^{4+} spin structure is not yet a well understood matter [26, 28]. It is a question whether the Ru^{4+} spin order has contribution to polarization or not, although our results exclude this possibility. Further studies on this point are recommended in future.

4 Conclusion

In conclusion, we have synthesized double pyrochlore oxide $Dy_2Ru_2O_7$ and investigated its multiferroic properties at low temperature. The pyroelectric current data indicate that $Dy_2Ru_2O_7$ has a ferroelectric transitions at $T_c \sim 18$ K and the measured polarization for polycrystalline samples at 2 K is about 145 $\mu C/m^2$. This polarization is believed to correlate with the spin relaxation above the Dy^{3+} spin ice like state at ~ 1.8 K. It is suggested that this spin relaxation is relevant with the Ru^{4+}–Dy^{3+} interactions and accommodates the magnetic monopole excitation which contributes to the ferroelectricity.

Acknowledgements This work was supported by the National Basic Research Program of China (973 Project) (Grant No. 2011CB922101), the National Natural Science Foundation of China (Grant Nos. 11234005, 11374147, and 51332006), and the Priority Academic Program Development of Jiangsu Higher Education Institutions, China.

References

1. S. T. Bramwell and M. J. P. Gingras, Spin ice state in frustrated magnetic pyrochlore materials, *Science*, 2001, 294: 1495
2. A. P. Ramirez, A. Hayashi, R. J. Cava, R. Siddgarthan, and B. S. Shastry, Zero-point entropy in "spin ice", *Nature*, 1999, 399: 333
3. J. S. Gardner, M. J. P. Gingras, and J. E. Greedan, Magnetic pyrochlore oxides, *Rev. Mod. Phys.*, 2010, 82: 53
4. L. Balents, Spin liquids in frustrated magnets, *Nature*, 2010, 464: 199
5. M. A. Subramanian, G. Aravamudan, and G. V. Subba Rao, Oxide pyrochlores – A review, *Prog. Solid State Chem.*, 1983, 15: 55
6. S. Rosenkranz, A. P. Ramirez, A. Hayashi, R. J. Cava, R. Siddharthan, and B. S. Shastry, Crystal-field interaction in the pyrochlore magnet $Ho_2Ti_2O_7$, *J. Appl. Phys.*, 2000, 87: 5914
7. R. G. Melko, B. C. den Hertog, and M. J. P. Gingras, Long-range order at low temperatures in dipolar spin ice, *Phys. Rev. Lett.*, 2001, 87: 067203
8. G. W. Chern, P. Mellado, and O. Tchernyshyov, Two-stage ordering of spins in dipolar spin ice on the Kagome lattice, *Phys. Rev. Lett.*, 2011, 106: 207202
9. J. D. M. Champion, A. S. Wills, T. Fennell, S. T. Bramwell, J. S. Gardner, and M. A. Green, Order in the Heisenberg pyrochlore: The magnetic structure of $Gd_2Ti_2O_7$, *Phys. Rev. B*, 2001, 64: 140407(R)
10. O. A. Petrenko, M. R. Lees, G. Balakrishnan, and D. McK. Paul, Magnetic phase diagram of the antiferromagnetic pyrochlore $Gd_2Ti_2O_7$, *Phys. Rev. B*, 2004, 70: 012402
11. T. Fennell, P. P. Deen, A. R. Wildes, K. Schmalzl, D. Prabhakaran, A. T. Boothroyd, R. J. Aldus, D. F. McMorrow, and S. T. Bramwell, Magnetic Coulomb phase in the spin ice $Ho_2Ti_2O_7$, *Science*, 2009, 326: 415

12. M. Ito, Y. Yasui, M. Kanada, H. Harashina, S. Yoshi, K. Murata, M. Sato, H. Okumura, and K. Kakurai, Nature of spin freezing transition of geometrically frustrated pyrochlore system $R_2Ru_2O_7$ (R=rare earth elements and Y), *J. Phys. Chem. Solids*, 2001, 62: 337
13. C. Bansal, H. Kawanaka, H. Bando, and Y. Nishihara, Structure and magnetic properties of the pyrochlore $Ho_2Ru_2O_7$: A possible dipolar spin ice system, *Phys. Rev. B*, 2002, 66: 52406
14. N. Taira, M. Wakeshima, and Y. Hinatsu, Specific heat and ac susceptibility studies on ruthenium pyrochlores $R_2Ru_2O_7$ (R=rare earths), *J. Solid State Chem.*, 2000, 152: 441
15. N. Taira, M. Wakeshima, and Y. Hinatsu, Magnetic susceptibility and specific heat studies on heavy rare earth ruthenate pyrochlores $R_2Ru_2O_7$ (R = Gd–Yb), *J. Mater. Chem.*, 2002, 12: 1475
16. S. W. Cheong and M. Mostovoy, Multiferroics: A magnetic twist for ferroelectricity, *Nat. Mater.*, 2007, 6: 13
17. K. F. Wang, J. M. Liu, and Z. F. Ren, Multiferroicity: The coupling between magnetic and polarization orders, *Adv. Phys.*, 2009, 58: 321
18. S. Dong and J. M. Liu, Recent progress of multiferroic perovskite manganites, *Mod. Phys. Lett. B*, 2012, 26: 1230004
19. J. M. Liu and C. W. Nan, Ferroelectricity and multiferroicity: Broader way to go beyond, *Front. Phys.*, 2012, 7(4): 373
20. A. P. Ramirez, B. S. Shastry, A. Hayashi, J. J. Krajewski, D. A. Huse, and R. J. Cava, Multiple field-induced phase transitions in the geometrically frustrated dipolar magnet: $Gd_2Ti_2O_7$, *Phys. Rev. Lett.*, 2002, 89: 067202
21. M. Tokunaga, Studies on multiferroic materials in high magnetic fields, *Front. Phys.*, 2012, 7(4): 386
22. X. W. Dong, K. F. Wang, S. J. Luo, J. G. Wan, and J.-M. Liu, Coexistence of magnetic and ferroelectric behaviors of pyrochlore $Ho_2Ti_2O_7$, *J. Appl. Phys.*, 2009, 106: 104101
23. D. Liu, L. Lin, M. F. Liu, Z. B. Yan, S. Dong, and J.-M. Liu, Multiferroicity in spin ice $Ho_2Ti_2O_7$: An investigation on single crystals, *J. Appl. Phys.*, 2013, 113: 17D901
24. L. Lin, Z. Y. Zhao, D. Liu, Y. L. Xie, S. Dong, Z. B. Yan, and J.-M. Liu, Chemically modulated multiferroicity in Dy-doped $Gd_2Ti_2O_7$, *J. Appl. Phys.*, 2013, 113: 17D903
25. D. I. Khomskii, Electric dipoles on magnetic monopoles in spin ice, *Nature Commun.*, 2012, 3: 904
26. C. R. Wiebe, J. S. Gardner, S.J. Kim, G. M. Luke, A. S. Wills, B. D. Gaulin, J. E. Greedan, I. Swainson, Y. Qiu, and C. Y. Jones, Magnetic ordering in the spin-ice candidate $Ho_2Ru_2O_7$, *Phys. Rev. Lett.*, 2004, 93: 076403
27. L. J. Chang, M. Prager, J. Perßon, J. Walter, E. Jansen, Y. Y. Chen, and J. S. Gardner, Magnetic order in the double pyrochlore $Tb_2Ru_2O_7$, *J. Phys.: Condens. Matter*, 2010, 22: 076003
28. M. Rams, A. Zarzycki, A. Pikul, and K. Tomala, Magnetic order and crystal field in $Dy_2Ru_2O_7$ and $Yb_2Ru_2O_7$, *J. Magn. Magn. Mater.*, 2011, 323: 1490
29. B. Lorenz, Y. Q. Wang, and C. W. Chu, Ferroelectricity in perovskite $HoMnO_3$ and $YMnO_3$, *Phys. Rev. B*, 2007, 76: 104405
30. N. Zhang, S. Dong, G. Q. Zhang, L. Lin, Y. Y. Guo, J.M. Liu, and Z. F. Ren, Multiferroic phase diagram of Y partially substituted $Dy_{1-x}Y_xMnO_3$, *Appl. Phys. Lett.*, 2011, 98: 012510
31. N. Zhang, S. Dong, and J.M. Liu, Ferroelectricity generated by spin–orbit and spin–lattice couplings in multiferroic $DyMnO_3$, *Front. Phys.*, 2012, 7(4): 408
32. K. Matsuhira, Y. Hinatsu, and T. Sakakibara, Novel dynamical magnetic properties in the spin ice compound $Dy_2Ti_2O_7$, *J. Phys.: Condens. Matter*, 2001, 13: L737